Reliability Engineering and System Safety 196 (2020) 106746

Contents lists available at ScienceDirect

Reliability Engineering and System Safety

journal homepage: www.elsevier.com/locate/ress

A novel generalized analytical reliability assessment method of smart grids including renewable and non-renewable distributed generations and plug-in hybrid electric vehicles

Ali-Mohammad Hariri[a], Hamed Hashemi-Dezaki[a,*], Maryam A. Hejazi[a]

[a] Department of Electrical and Computer Engineering, University of Kashan, 6 km Ghotbravandi Blvd, Kashan 8731753153, Iran

ARTICLE INFO

Keywords:
Reliability evaluation
Uncertainty
Smart grid
Generalized analytical method
Renewable and non-renewable distributed generation (DG)
Plug-in hybrid electric vehicle (PHEV)
Well-being assessment

ABSTRACT

Because of the importance of smart grids reliability, various stochastic-based simulation methodologies e.g. Monte Carlo simulation (MCS) have been developed. In contrast, the much less effort has been devoted in literature to develop the generalized analytical ones. In this paper, a new generalized analytical methodology is developed for smart grids' reliability assessment. The main contributions of this article are proposing a new state matrix (S-matrix) method including the novel model for investigating the smart grid operating modes by using the segmentation concepts and graph theory; developing a new comprehensive model of PHEVs considering the all their uncertainties; and introduction of a novel integrating methodology of separate elements.

The proposed method is applied to the IEEE 33-bus test system. The comparison of test results and those of MCS-based methods and also with other available analytical methods illustrate the accuracy of the proposed method. The sensitivity analyses results imply that the proposed method is not adversely affected due to changes in different uncertain parameters.

1. Introduction

1.1. Motivation and incitement

The annual average of 1.3% increment (from 2016 to 2040) in the world energy demand has been estimated [1,2]. In BP Energy Outlook 2030 [2], it has been reported that the fastest growth rate (annual average of 7%) belongs to renewable energies from 2018 to 2040. In addition, according to BP Energy outlook 2030 [1], about 30% of car passengers vehicle kilometers is provided by electricity in 2040. On the other hand, according to the international renewable energy agency (IRENA) report [3], the significant decrease in renewable energy cost such as an 81% decrease in solar photovoltaic module costs has occurred, and therefore the use of these energies. Hence, it is inevitable to the deployment of the smart grid including wind turbine and photovoltaic distributed generation (DG) units and the battery electric vehicles (BEVs) or plug-in hybrid electric vehicles (PHEVs).

Because of the stochastic behavior of renewable DG units, PHEVs, and other uncertain elements, the smart grid designing based on reliability and economic aspects is not easy. In recent years, a wide variety of smart grid reliability evaluation methods been proposed. Much effort has been devoted in literature to propose the stochastic simulation methods for reliability evaluation of smart grids. Since the stochastic simulation methods such as Monte Carlo simulation (MCS) are capable to overcome the uncertainty modeling problems [4–6], the most available approaches related to reliability evaluation of smart grids have been developed by using the MCS. Although by using the MCS, it is possible to model and study the probabilistic and stochastic behaviors of uncertain elements, it would be time-consuming. Hence, it is interesting to propose a novel analytical method with the desired accuracy which supports all uncertainties of smart grids' reliability assessment in the widespread presence of renewable energy resources and PHEVs. Nevertheless, less attention has been paid to this subject.

Reliability evaluation of smart grids with a reasonable computing time and the desired accuracy level is interesting. The importance of developing a fast and precise reliability evaluation method is highlighted when the heuristic-based optimization algorithms are used to solve the reliability-based optimization problems or other reiterative studies of smart grids are concerned. Moreover, developing a fast and accurate generalized analytical reliability method would be useful for reliability-based operation or short-term planning decision making processes.

* Corresponding author.
E-mail addresses: am.hariri@grad.kashanu.ac.ir (A.-M. Hariri), hamed.hashemi@kashanu.ac.ir, hamed.hashemi@gmail.com (H. Hashemi-Dezaki), mhejazi@kashanu.ac.ir (M. A. Hejazi).

https://doi.org/10.1016/j.ress.2019.106746
Received 9 January 2019; Received in revised form 7 September 2019; Accepted 10 November 2019
Available online 11 November 2019
0951-8320/

Nomenclature

m_n	Number of states of the nth element
S_n	The state matrix (S-Matrix) of the nth element
$x_{n,\ i}$	The i-th state of the nth element
$\Pr_{n,i}$	The i-th state probability of the nth element
$F(x)$	The cumulative density function (CDF) of stochastic variable "x"
$f(x)$	Probability density function (PDF) of stochastic variable "x"
$\mu,\ \sigma,\ \sigma^2$	Mean value, standard deviation, and variance of any stochastic parameter based on the historical data
$TDES$	The state matrix of time-dependent elements (TDEs) e.g. photovoltaic (PV) distributed generation (DG) units, conventional loads, and plug-in hybrid electric vehicles (PHEVs) charging load demand which represents the aggregated surplus or shortage power and its corresponding probability of any segment
v	Instantaneous wind speed (m/s)
$P_{WT}(v)$	The output power of wind turbine (WT)-based DG units as a function of wind speed (W)
$P_{WT-rated}$	The rated output power of WT-based DG unit (W)
v_{cut-in}, v_{rated}, $v_{cut-off}$	Cut-in, rated, and cut-off wind speed of the WT-based DG unit (m/s)
$A,\ B,\ C$	Specific coefficients of the WT-based DG unit characteristics as functions of the wind speed
$A_n,\ U_n$	Availability and unavailability probability of the nth element
$N_{PV-Modules}$	Number of PV modules
N_{Buses}	Number of system buses
N_{DGs}	Number of DG units
N_{lines}	Number of distribution lines
N_{WT}	Number of WT DG units
N_{PV}	Number of PV DG units
N_{NRES}	Number of non-renewable energy source (NRES) DG units
N_{Tr}	Number of substation transformers
N_{seg}	Number of system segments
N_{PS}	Number of PHEV states
$N_{PHEV-types}$	Number of PHEV types
$N_{Configs}$	Number of system topologies and operation modes
$N_{WT}^{seg_r}$	Number of the WTs' states of the rth segment
$N_{TDE}^{seg_r}$	Number of the TDEs' states of the rth segment
k_t	Solar clearness index
$\alpha,\ \beta$	Shape parameters of the Beta probability distribution function
P_{PV}	The output power of PV-based DG unit (W)
PVS	PV state matrix
τ	Number of time interval in each hour, which can be defined for PV-based DG units, PHEVs arrival time, and PHEVs departure time
$k_t^{\min}$, $k_t^{\max}$	The minimum and maximum value of the solar clearness index
$P_{NRES-rated}$	The rated output power of NRES-based DG unit (W)
$P_{Tr-rated}$	The rated power capacity of the main substation's transformer (W)
Seg_i	The i-th segment
CC	Matrix of connected components in order to determine the system segments and operation modes of the smart grid
$conncom$	Connected component function based on graph theory concepts
LP_i	The i-th load point
$SEGG$	Segmented graph
$Area_j$	The j-th area of the system
$N_{Area}^{\max}$	Maximum number of separated areas of the smart grid due to the operating of protective or switching devices
$\Pr_{SEGG}^{r}$	Probability of the r-th segmented graph of the system
CS_i	The connected segments' matrix of the system due to any fault in the i-th segment
AT	PHEV arrival time matrix
$AT^{\min}$	The minimum value of the historical arrival times
$AT^{\max}$	The maximum value of the historical arrival times
τ_{AT}	Number of time interval in each hour for PHEVs arrival time
DT	PHEV departure time matrix
$DT^{\min}$	The minimum value of the historical departure times
$DT^{\max}$	The maximum value of the historical departure times
τ_{DT}	Number of time interval in each hour for PHEVs departure time
DD	PHEV driving distance matrix
$DD^{\min}$	The minimum value of the historical driving distances
$DD^{\max}$	The maximum value of the historical driving distances
m_{DD}	Number of the PHEVs driving distances' states
PSM_q	The q-th PHEVs' state matrix
$\Pr_{type}^{r}$	Probability of the r-th PHEV type
$SOC_r^{\max}$	The maximum state of charge (SOC) of the r-th PHEV type
$SOC_{initial}$	The initial value of the PHEV SOC
BC_r, $ECPK_r$	The battery capacity and energy consumption per kilometer (ECPK) of the r-th PHEV type
R_{Chg}	Charging level of the PHEV
$BV_{AT}(q,\ t)$	The q-th Boolean variable regarding the PHEVs arrival time which represents that the PHEVs could be charged in the tth time interval or could not.
$BV_{DT}(q,\ t)$	The qth Boolean variable regarding the PHEVs departure time which represents that the PHEVs could be charged in the t-th time interval or could not.
$BV_{SOC}(q,\ t)$	The q-th Boolean variable regarding the PHEVs state of charge (SOC) which represents that the PHEVs could be charged in the t-th time interval or could not.
$PCLM$	PHEV charging load matrix
SS	System state which determines the state of the system as a function of its subsystems
$BV_{Constraints}^{q}$	The Boolean variable regarding all system constraints such as power flow limits of the q-th system state
$EENS^q$, $EENS$	The expected energy not-supplied (EENS) of the qth system state and the whole system EENS
k_{wind}, c_{wind}	Weibull shape and scale parameters of wind speed
P_{MS}	Supplied power of the main substation
P_{DGs}	Supplied power of DG units
P_{load}	The demand for conventional loads
P_{PHEVs}	The demand for PHEVs' charging load demand
$V_{q,\ i}$, $\delta_{q,\ j}$	Magnitude and angle of the voltage of the ith load point under the q-th system state
Y_{ij}, θ_{ij}	Magnitude and phase angle of the ith row and jth column's element of the admittance matrix
P_l, $P_{\max,\ l}$	Transmitted power passing through the lth distribution line and the transmission power limit of the i-th line
f, $f_{\min}$, $f_{\max}$	System frequency and the upper and lower bounds of the permitted frequency
$V_{q,\ i}$, $V_{\min}$, $V_{\max}$	Voltage magnitude of the ith load point under the qth system state and the upper and lower bounds of the permitted voltage
n_{bus}	Number of system load points
$BV_{voltage-profile}^{q}$	The Boolean variable regarding the voltage profile of the smart grid under the q-th system state
$BV_{P-lines}^{q}$	The Boolean variable regarding the power passing through the distribution lines under the q-th system state
BV_{P-DGs}^{q}	The Boolean variable regarding the power generation of the DG units in the qth system state
P_{line-i}, $P_{line-i}^{\max}$	Power passing through i-th line and the maximum transmittable power of ith line

$P_{G,\ g}$	The power generation of g-th DG unit		like NRES DGs to renewable ones
$P_{G,g}^{\min}$	The minimum power generation of gth DG unit	R_{AT}	Range of each discretized arrival time interval
$P_{G,g}^{\max}$	The maximum power generation of gth DG unit	R_{DT}	Range of each discretized departure time interval
P_{DDG}	The output power of controllable and dispatchable DG units	R_{DD}	Range of each discretized driving distance interval
K_{D2R}	The Ratio of power generation of controllable DG units		

The core research work of this paper is focusing on the development of a generalized analytical reliability evaluation method which considers the different uncertainties. Achieving the desired accuracy of the reliability calculations is another aim of this research in addition to the decrease in the computing time of smart grids reliability evaluation.

1.2. Literature review

Atwa et al. [7,8] proposed the MCS and analytical techniques in order to evaluate the reliability of the distribution systems including wind/solar DG units. The authors claimed that there is no considerable difference between the results obtained by the technical approach and MCS. Although the main concepts related to the analytical technique of reliability evaluation have been clearly explained in [7,8], there is a gap to introduce a comprehensive mathematical model for integrating the different elements. Moreover, the authors have not presented any solution about the PHEVs and other uncertain elements in the demand side. Similar research was conducted in [9]. Moeini-Aghtaie et al. [9] presented a generalized approach in order to determine the reliability of energy hubs and smart grids including PHEVs. In [9], the modeling of the PHEVs under different operation scenarios such as vehicle to grid (V2 G) mode and studying their various impacts on the energy hub reliability have been concerned. The detailed analytical technique and mathematical model about the reliability evaluation model as well as analyzing the different impacts of PHEVs on the energy hubs don't exist in [9]. In addition, the presented method of [9] has not been validated by other approaches e.g. MCS. It was found in [10,11] that by probability table (P-table) approach as an analytical method, it is possible to evaluate the reliability of smart grids based on cyber-power interdependencies. Nevertheless, in [10,11], there is no solution for modeling uncertain elements such as renewable DG units, PHEVs, and so on. To overcome this problem, the second author of this article et al. [12–14] proposed MCS-based methods to evaluate the reliability of the smart grid considering the cyber-power interdependencies. Although some researches such as [7–11] tried to propose the analytical reliability evaluation technique of smart grid, there is a knowledge gap about developing a comprehensive analytical technique. Until now, no comprehensive mathematical model has been developed to assess the smart grids' reliability which simultaneously considers all uncertainties of supply and demand sides.

1.3. Contributions and paper organization

This article tries to fill such a knowledge gap explained in the literature review by contributing to propose a new mathematical model in order to comprehensive analytical reliability assessment of smart grid, which considers all uncertainties. The proposed method is developed based on the convolution of probability distributions. In this paper, the probabilistic state of any element is modeled based on the state matrix (S-Matrix). The state matrix consists of all states of any element and their probability values. Generally, the continuous uncertain parameters and characteristics of any element are discretized, and the probability of any of these discretized states is calculated.

Creating the state matrices of subsystems based on the convolution of probability distributions and their aggregations play the most important roles. The novelties of creating the state matrix of the PHEVs are more important than those of other subsystems like DG units because less attention has been devoted to the literature to an analytical model of PHEVs.

Another challenging issue in the analytical reliability evaluation of the smart grid is related to different network topologies based on contingency analyses. By using the graph theory and its combination to the segmentation concept [8,15,16], it is possible to create the state matrix of the system configuration and topology. In the proposed method, the generalized integration modeling of all S-matrices is provided. Furthermore, by using the proposed method, it is possible to evaluate the well-being indices (healthy, marginal, and at-risk probability) in addition to conventional reliability and adequacy indices such as loss of load expected (LOLE), expected energy not supplied (EENS), etc.

The most important contributions of this paper are related to the reliability evaluation of smart grids as follows:

1) Mathematical reliability modeling of renewable DG units such as wind/photovoltaic-based DG units based on State matrix;
2) Mathematical reliability modeling of PHEVs which considers all PHEVs' uncertainties based on vehicle drivers' behaviors;
3) Proposing the state matrix-based modeling of smart grid topology and configuration according to contingency analyses by using the graph theory and segmentation concepts [8,15,16];
4) Proposing an integration model of smart grid reliability evaluation based on the state matrix of any element;
5) Validating the new proposed generalized analytical reliability

Table 1
List of smart grid stochastic variables

Element	Variable name	Variable type	Source of uncertainty
Wind DG unit	WT output power	Continuous	Various electrical or mechanical failures/ wind speed
PV DG unit	PV output power	Continuous	Various electrical or mechanical failures/ solar irradiance/ambient temperature
NRES DG unit	Availability	Binary	Various electrical or mechanical failures
PHEVs' charging load demand	Arrival time	Continuous	PHEVs' owners' behaviors
	Departure time	Continuous	PHEVs' owners' behaviors
	Driving distance	Continuous	PHEVs' owners' behaviors
	PHEV type	Integer	Manufacturers' specifications
Electrical load	Load value	Continuous	Load variation
Distribution lines	Availability	Binary	Various electrical or mechanical failures
Distribution transformers	Availability	Binary	Various electrical or mechanical failures
Circuit breakers/switches	Appropriate performance	Binary	Various electrical or mechanical failures

evaluation method of smart grids based on the comparison of the obtained results and those of MCS-based methods;
6) Evaluating the well-being indices (healthy, marginal, and at-risk probability) by use of the proposed method in addition to conventional reliability indices.

This paper is organized as follows. Section II addresses the modeling of wind turbine DG units, PV-based DG units, non-renewable DG units, system topologies and its operation modes, and PHEVs. Section III discusses the test results, and the conclusions are explained in Section IV.

2. Modeling

In Table 1, the list of considered stochastic variables has been presented. In this section, the modeling of each element and subsystem is proposed.

2.1. Modeling of Wind Turbine (WT) DG Units

In the proposed methodology, for any uncertain element of the smart grid such as wind turbine DG units, a state matrix (S-Matrix) element is created as shown in (1).

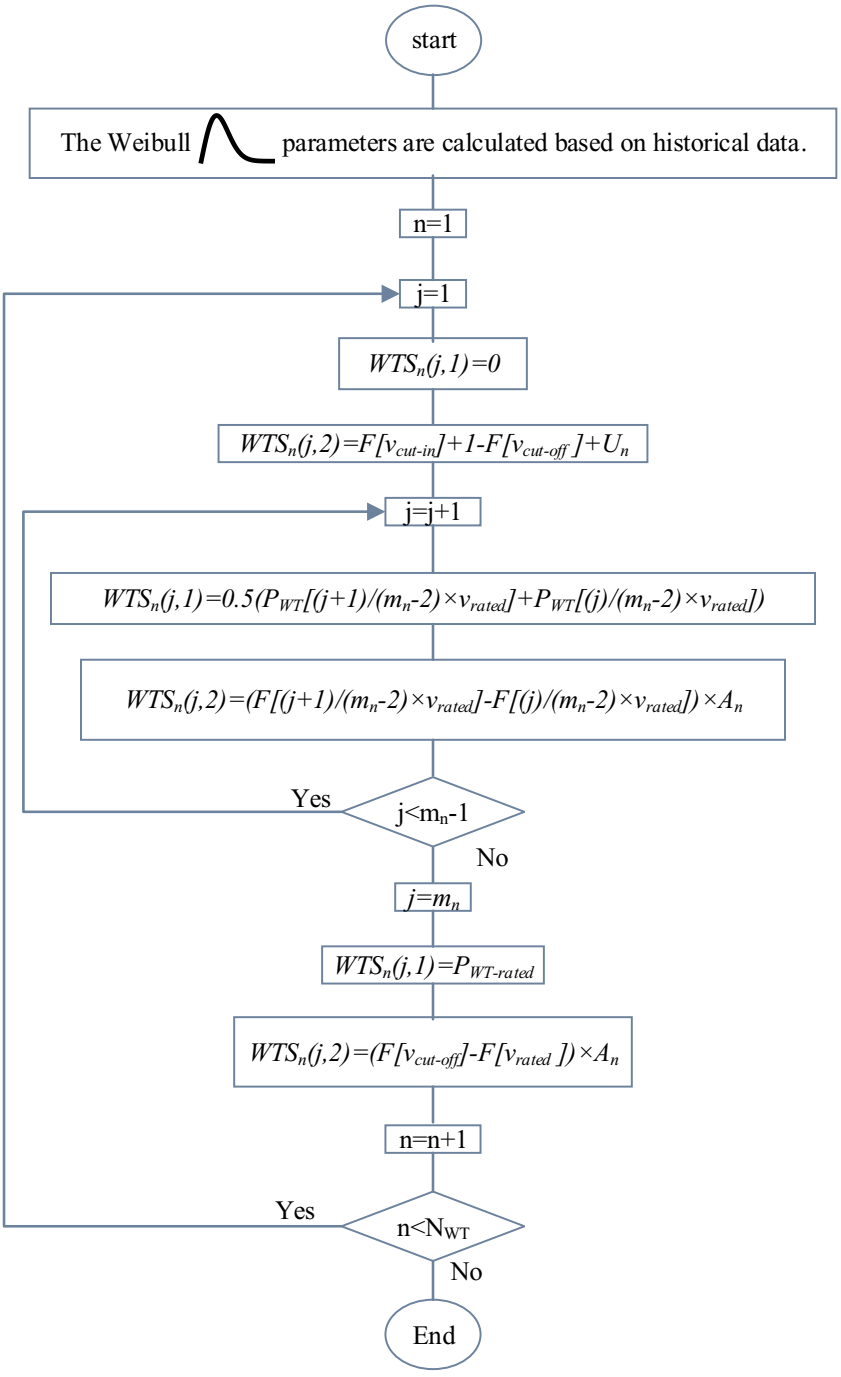

Fig. 1. Flowchart of WT DG units S-Matrix production

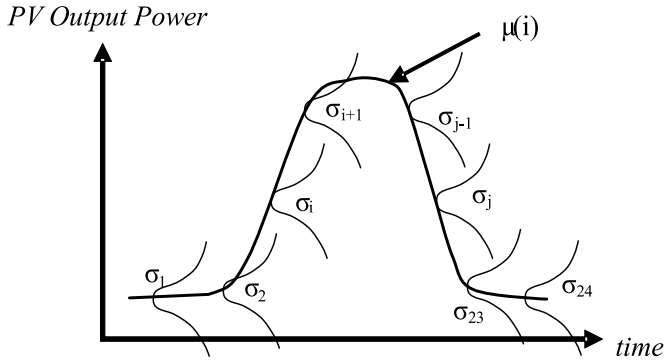

Fig. 2. Daily PV DG unit output power generation

$$S_n = \begin{bmatrix} x_{n,1} & Pr_{n,1} \\ x_{n,2} & Pr_{n,2} \\ \vdots & \vdots \\ x_{n,i} & Pr_{n,i} \\ \vdots & \vdots \\ x_{n,(m_n-1)} & Pr_{n,(m_n-1)} \\ x_{n,m_n} & Pr_{n,m_n} \end{bmatrix}_{m_n \times 2} \quad \forall\, n \in 1{:}\, N \tag{1}$$

The m represents the number of states for the n-th sub-system of the smart grid. Each element in the first column of S-Matrix ($x_{n,\ i}$) represents the i-th state of the n-th element and $Pr_{n,i}$ is its corresponding probability.

To create the S-Matrix of the wind turbine DG units, it is essential to determine the different output power of these renewable DG units as a

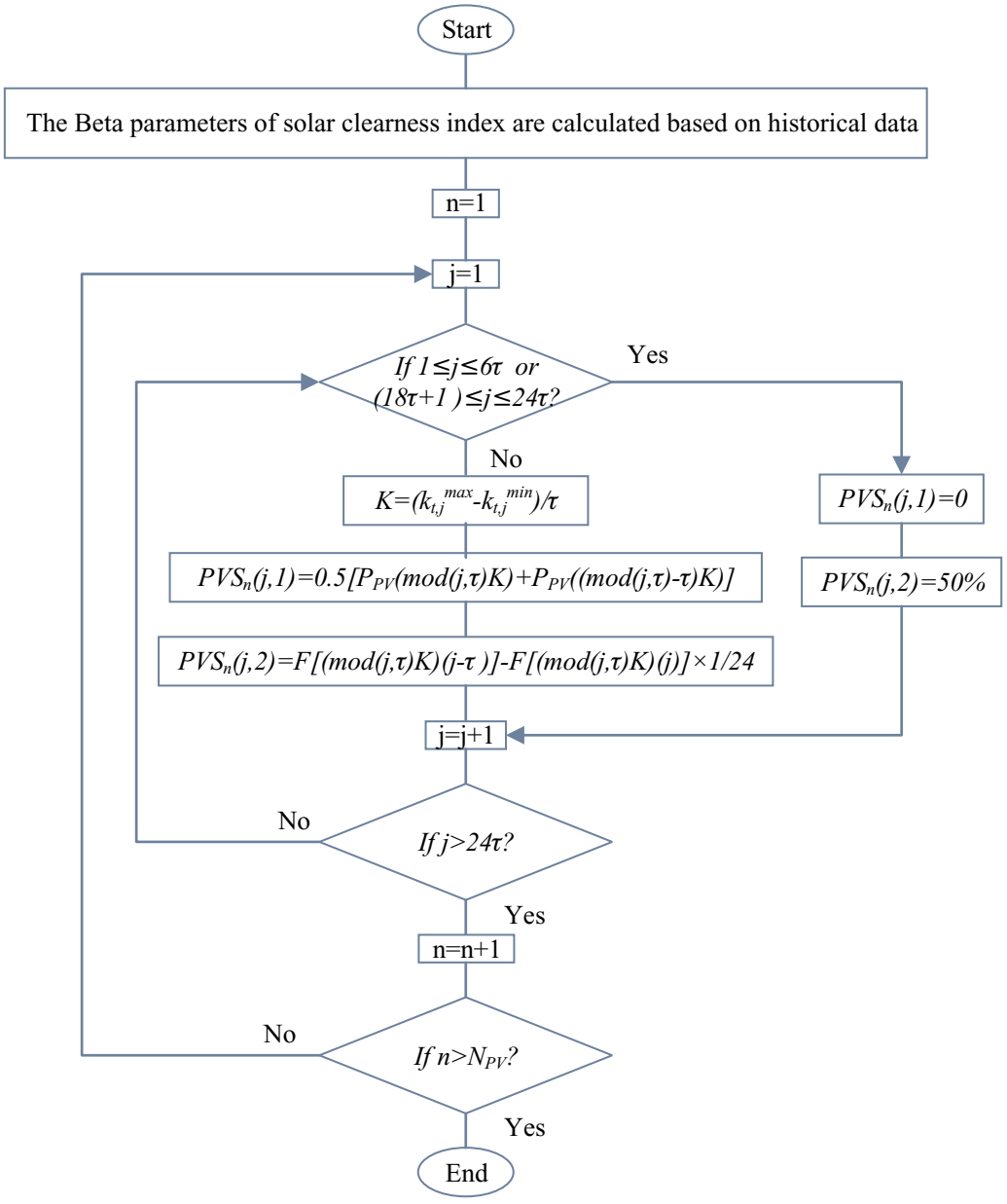

Fig. 3. Flowchart of PV DG units S-Matrix production.

function of various wind speeds which can be mathematically formulated as (2) [17,18].

$$P_{WT}(v)=\begin{cases}P_{WT-rated}\times(A+B\times v+C\times v^2) & v_{cut-in}<v<v_{rated}\\ P_{WT-rated} & v_{rated}<v<v_{cut-off}\\ 0 & otherwise\end{cases} \quad (2)$$

where the defined parameters, e.g. A, B, and C can be determined based on (3-5) [17,18]:

$$A=\frac{1}{(v_{cut-in}-v_{rated})^2}\times\left[v_{cut-in}(v_{cut-in}+v_{rated})-4v_{rated}v_{cut-in}\left(\frac{v_{cut-in}+v_{rated}}{2v_{rated}}\right)^3\right] \quad (3)$$

$$B=\frac{1}{(v_{cut-in}-v_{rated})^2}\left[\begin{matrix}4(v_{cut-in}+v_{rated})\left(\frac{v_{cut-in}+v_{rated}}{2v_{rated}}\right)^3\\ -(3v_{cut-in}+v_{rated})\end{matrix}\right] \quad (4)$$

$$C=\frac{1}{(v_{cut-in}-v_{rated})^2}\left[2-4\left(\frac{v_{cut-in}+v_{rated}}{2v_{rated}}\right)^3\right] \quad (5)$$

The output generation of WT for wind speed between the rated and cut-off values is equal to rated power. When the wind speed is less than the cut-in speed or exceeds the cut-off value, the output generation will be zero. Furthermore, according to the formula given in (2–5), there is a second-order polynomial function between the output generation and wind speed.

Moreover, in some references, the easier formula with a linear [19] or a cubic [20,21] relationship between the output power and the wind speeds between the cut-in and rated values have been used to calculate the output power of the WT-based DG units. By using the (3–5), the little more accurate calculations can be obtained.

The output generated of WT for wind speed between the rated and cut-off values is equal to the rated power. When the wind speed is less than the cut-in speed or exceeds the cut-off value, the output power will be zero. Furthermore, according to the formula given in (2), there is a second-order polynomial function between the output generated and the wind speed for other conditions.

To produce the S-Matrix of the WT DG units, it is essential to discretize the states of WT output power as given in (6).

$$x_{n,j}=WTS_n(j,1)=\begin{cases}0 & j=1\\ \dfrac{\left[P_{WT}\left(\frac{(j+1)}{(m_n-2)}v_{rated}\right)+P_{WT}\left(\frac{j}{(m_n-2)}v_{rated}\right)\right]}{2} & j=2:m_n-1\quad\forall n\in\{WT\}\\ P_{WT-rated} & j=m_n\end{cases} \quad (6)$$

where $m_n$represents the number of states of the wind turbine DG unit output power.

When the WT is out-of-service due to any failure or the wind speed is less than cut-in speed or exceeds the cut-off speed, the first state occurs. Hence, the probability of the first state should be calculated by using the cumulative density function (CDF) of wind speed. Generally, the probability value of any speed range can be calculated.

The last (them_nth) state of WT output power is similarly calculated. If the WT is in-service, and the wind speed is in range of the rated speed up to cut-off speed, the output power will be equal to the WT rated power. Accordingly, this state probability is determined by multiplying the WT availability probability and the desired wind speed probability together.

Because of the WT output power curve for wind speed from the cut-in to cut-off speed, it is necessary to discretize the WT output power in this division. The total number of states for this division is (m_n-2). So, the output power range is divided into(m_n-2)states.

A wide variety of probability density functions (PDFs) has been reported for modeling the stochastic behavior of wind, but the Weibull distribution function is more well-known and common than others [21–23]. Moreover, the Weibull cumulative distribution function ($F(v)$) can be easily calculated by using (7) [24–26].

$$F(v)=1-\exp\left[\left(-\frac{v}{c_{wind}}\right)^{k_{wind}}\right] \quad (7)$$

The probability of any discussed state can be investigated as (8). In addition, the mean values of the lower and upper bounds are assigned for the state value.

$$Pr_{n,j}=WTS_n(j,1)=\begin{cases}[F(v_{cut-in})-0]+[1-F(v_{cut-off})]+U_n & j=1\\ \left[F\left(\frac{(j+1)}{(m_n-2)}v_{rated}\right)-F\left(\frac{j}{(m_n-2)}v_{rated}\right)\right]\times A_n & \\ \quad j=2:m_n-1\ \forall n\in\{WT\} & \\ [F(v_{cut-off})-F(v_{rated})]\times A_n & j=m_n\end{cases} \quad (8)$$

The development of the S-Matrix for renewable DG units such as WT/PV DG units is the novelty of this paper regarding the reliability modeling of these stochastic DG units. The available models for calculating the output power of these DG units are used to develop the proposed analytical reliability evaluation method.

In Fig. 1, the flowchart of WT DG unit S-Matrix production is depicted.

2.2. Modeling of PV DG Units

The PV DG unit output power is calculated as a function of the ambient temperature and the solar irradiance [27–29]. By determining the clearness index, the ambient temperature, and the PV module specifications, the PV DG unit output power can be calculated as equations reported in [30].

A wide variety of PDFs have been proposed for solar clearness index based on the historical data [31,32]. However, the Beta distribution function is the most popular [33–36]. Hence, the Beta distribution function is used for investigating the clearness index as given in (9) and (10).

$$f(k_t)=\frac{k_t^{(\alpha-1)}(1-k_t)^{(\beta-1)}}{B(\alpha,\beta)} \quad (9)$$

$$B(\alpha,\beta)=\frac{\Gamma(\alpha)\Gamma(\beta)}{\Gamma(\alpha+\beta)} \quad (10)$$

By using the historical data, the mean value and the standard deviation or variance value of the clearness index can be investigated. Therefore, to discretize the states of the PV output power, it is essential to divide the time into 15-min or 60-min intervals [37]. Moreover, the range of the clearness index at any interval time as shown in Fig. 2 should be discretized.

The State matrix of the PV DG unit can be produced as described in (11) and (12). The probability of any state is determined by using the Beta cumulative distribution function. In order to simplify the PV DG unit S-Matrix creating, it is assumed that the temperature is constant and equal to that time segment average temperature. This assumption is reasonable because the rate of change of temperature is not high.

According to the proposed reliability evaluation method based on the S-Matrix, it has been assumed that from 6:00 PM up to 6:00 AM and their corresponding time segments, the output power of PV DG units is zero. For other times, the states of the clearness index are discretized into the τstates. The PV DG units' output power of the upper and lower bounds of any discussed states are calculated. The average of the output power of the lower and upper bounds is assigned to the corresponding state value.

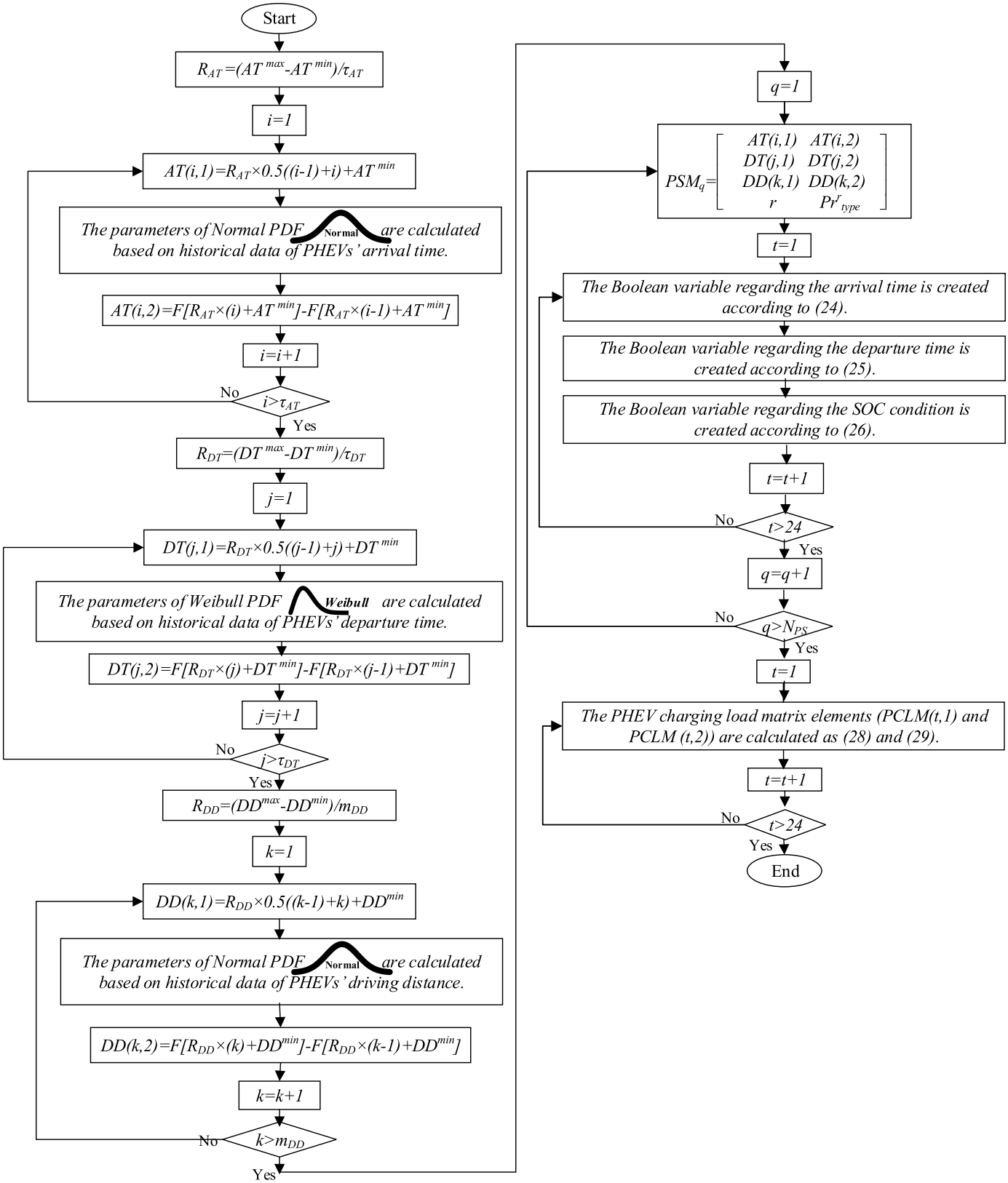

Fig. 4. Flowchart of the proposed method for modeling the PHEVs charging load demand.

$$x_{n,j} = PVS_n(j,1) = \begin{cases} 0 & j = 1{:}\ 6\tau or (18\tau+1){:}\ 24\tau \\ \left[P_{PV}\left(\frac{mod(j,\tau)}{(\tau)}(k_{t,j}^{\max} - k_{t,j}^{\min})\right) + P_{PV}\left(\frac{[mod(j,\tau)-1]}{(\tau)}(k_{t,j}^{\max} - k_{t,j}^{\min})\right) \right] & \forall n \in \{PV\} \\ \hline 2 & 6\tau+1 \le j \le 18\tau \end{cases} \quad (11)$$

The probability of any state of PV DG units can be investigated as (12). As can be seen, the probability of any states corresponding to time segments between 6:00 PM and 6:00 AM would be equal to $\frac{1}{24\tau}$. The probability of other states would be calculated by using the clearness index's cumulative density function.

$$Pr_{n,j} = PVS_n(j,2) = \begin{cases} \frac{1}{24\tau} & j = 1{:}\ 6\tau or (18\tau+1){:}\ 24\tau \\ \left[F\left(\frac{mod(j,\tau)}{(\tau)}(k_{t,j}^{\max} - k_{t,j}^{\min})\right) - F\left(\frac{[mod(j,\tau)-1]}{(\tau)}(k_{t,j}^{\max} - k_{t,j}^{\min})\right) \right] \times \frac{1}{24} & 6\tau+1 \le j \le 18\tau \quad \forall n \in \{PV\} \end{cases} \quad (12)$$

Similar to the proposed S-Matrix mathematical model for the WT DG units, the available models of the PV DG units' output power calculation are utilized for creating the S-Matrix.

In Fig. 3, the flowchart of PV DG units' S-Matrix creating is shown.

2.3. Modeling of Nonnon-Renewable DG Units

The output power of non-renewable energy sources (NRES) is under control and can be dispatched. The NRES DG unit State matrix is calculated based on its availability and unavailability as (13). The exponential PDF [38] is used for the calculation of availability and unavailability of these DG units.

$$S_n = \begin{bmatrix} x_{n,1} = 0 & P_{n,1} = U_n \\ x_{n,2} = P_{NRES-rated} & P_{n,2} = A_n = (1-U_n) \end{bmatrix}_{(m_n=2)\times 2} \quad \forall n \in \{NRES\} \quad (13)$$

2.4. Modeling of Main main Substation

Usually, the main high voltage/ medium voltage (HV/MV) substation (MS) of any smart distribution grid includes greater than or equal to 2 transformers. On the other hand, the behavior of the main substation is not stochastic. Accordingly, the MS's State matrix can be developed as (14) and (15).

$$x_{n,j} = \begin{cases} (N_{Tr}-j) \times P_{Tr-rated} & j = 1{:}\ N_{Tr} \\ (N_{Tr}) \times P_{Tr-rated} & j = 1{:}\ N_{Tr}+1 \end{cases} \quad \forall n \in \{MS\} \quad (14)$$

$$\Pr_{n,j} = \begin{cases} \left(\frac{N_{Tr}}{j}\right) \times U_{Tr}^{j} \times A_{Tr}^{(N_{Tr}-j)} & j = 1{:}\ N_{Tr} \\ A_{Tr}^{N_{Tr}} & j = N_{Tr}+1 \end{cases} \quad \forall n \in \{MS\} \quad (15)$$

If the MS has the N_{Tr}transformers, the number of j-combinations can be calculated by using (16) which represents that the j number of transformers are out-of-service.

$$\left(\frac{N_{Tr}}{j}\right) = \frac{N_{Tr}!}{(N_{Tr}-j)!j!} \quad (16)$$

2.5. Modeling of Smart Grid Topology and Configuration

Based on the segmentation concepts [8,15,16], all elements including the load points (LPs), transmission lines, buses, etc., which are located in the downstream of a protective device experience the similar interrupts. In this paper, a novel methodology is proposed for modeling the smart grid topology based on the graph theory and segmentation concepts [8,15,16]. While any segment experiences a fault, the upstream protective devices operate. In addition, the downstream protective or switching device should be opened to isolate the faulty area. Hence, to modify the input/output matrix of the system due to any fault in each segment and to model the discussed tripping operating of the protective devices and opening of switching devices, the corresponding edges between the faulty segment and its neighbors should be removed as (17) and (18). Moreover, the separate areas in the new segmented graph of the smart grid by using MATLAB function "***conncom***" are detected as (19) and (20). In (21), the probability of any configuration and operation mode is calculated.

$$\begin{aligned} &If\ \ Seg_i\ is\ out-of-service. \\ &SEGG_{new}(k,1)|_{\forall k \ni SEGG(k,1)=Seg_i} = SEGG(k,2) \end{aligned} \quad (17)$$

$$\begin{aligned} &If\ \ Seg_i\ is\ out-of-service. \\ &SEGG_{new}(k,2)|_{\forall k \ni SEGG(k,2)=Seg_i} = SEGG(k,1) \end{aligned} \quad (18)$$

$$CS_i = conncom(SEGG_{new}) \quad (19)$$

$$Seg_l \in \{Area_j\} \quad \forall l \ni CS_i(l) = j \,\&\, \forall j = 1{:}\ N_{Area}^{\max} \quad (20)$$

$$\Pr_{SEGG}^{r} = \prod_{k=1}^{N_{seg}} A_k^{(x_k)} U_k^{(1-x_k)} \quad (21)$$

2.6. Modeling of PHEVs Charging Load

The PHEVs' characteristics are generally categorized into two types [39]: the characteristics based on their manufacturing data and electric grid constraints, and the uncertain characteristics of the EV owners' behaviors, respectively. In this paper, a comprehensive model considering both discussed characteristics is proposed.

The home arrival time is one important parameter in modeling the PHEVs charging load demand. The arrival time is a stochastic parameter that is normally distributed [12,40,41], and the State matrix of the arrival time as a subdivision of the State matrix of the PHEVs charging load can be initialized by using the normal PDF. The range of arrival time is divided into some time intervals. The average of the upper and lower bounds of any time interval is determined as a state of the arrival time. The corresponding probability of any state of the arrival time is calculated based on (22) by using the normal probability distribution function.

$$\begin{aligned} &AT(j,2) = Pr_{AT,j} = \\ &F\left[AT^{\min} + \frac{(AT^{\max} - AT^{\min})}{\tau_{AT}}(j)\right] \\ &- F\left[AT^{\min} + \frac{(AT^{\max} - AT^{\min})}{\tau_{AT}}(j-1)\right] \quad j = 1{:}\ \tau_{AT} \end{aligned} \quad (22)$$

Another important parameter of the modeling of PHEVs is the departure time. The charging duration is limited at first by the EV departure time. Since most EV owners leave home at a specific time in the morning, the Weibull PDF is more matches to the historical data of departure time than others [12,42]. All procedures of modeling the departure time State matrix is similar to those of arrival time, except the

probability density function. The PHEV is charged between the arrival and departure time until the SOC is less than the maximum permissive SOC. In order to evaluate the different probable SOC at arrival time, it is necessary to determine the initial SOC (when leaves the home or office) and the driving distance [43]. The probability distribution function of daily driving distance is assumed to be Normal [12,44]. Accordingly, the State matrix of the driving distance can be calculated by (23).

$$DD(j,2) = Pr_{DD,j} = F\left[DD^{\min} + \frac{(DD^{\max} - DD^{\min})}{m_{DD}}(j)\right] - F\left[DD^{\min} + \frac{(DD^{\max} - DD^{\min})}{m_{DD}}(j-1)\right] \quad j = 1: m_{DD} \tag{23}$$

The Boolean variables according to constraints for charging the

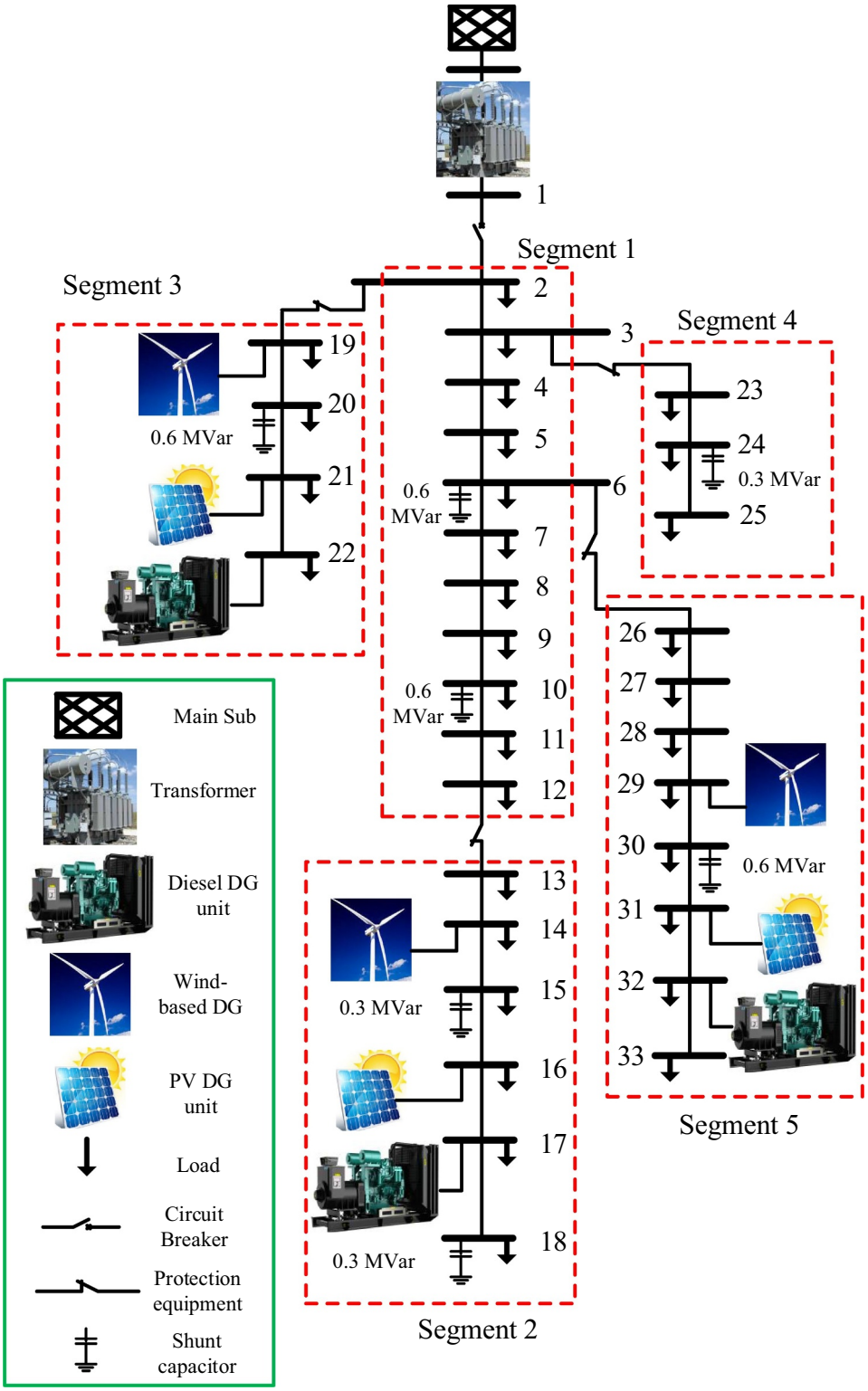

Fig. 5. The single line diagram of IEEE 33-bus test system [35].

PHEVs are defined as (24)–(27). The charging load of any time might not be zero when it is greater than the home arrival time and less than the departure time. In addition, it is necessary for PHEVs' charging that the PHEV state of charge (SOC) was less than the maximum permissive SOC. Otherwise, the PHEVs don't receive the electric power for charging. In Fig. 4, the flowchart of PHEV reliability modeling is shown.

In this paper, developing a novel mathematical model to evaluate the smart grids reliability evaluation has been concerned. It has been assumed that the PHEVs are unmanaged charging. The development of an extended model which considers the controls and management of the PHEVs charging is one of our future works. The proposed method would be flexible and can be extended to the modeling of the PHEVs charging management algorithms based on the state matrix and the convolution of probabilities.

$$BV_{AT}(q,t)=\begin{cases}1 & t \geq AT(i,1) \quad \forall\, t \in \{1,2,...,24\},\ i=1:\tau_{AT}\\ 0 & Otherwise. \quad \forall\, q \in \{1,2,...,N_{PS}\}\end{cases} \tag{24}$$

$$BV_{DT}(q,t)=\begin{cases}1 & t < DT(j,1) \quad \forall\, t \in \{1,2,...,24\},\ j=1:\tau_{DT}\\ 0 & Otherwise. \quad \forall\, q \in \{1,2,...,N_{PS}\}\end{cases} \tag{25}$$

$$BV_{SOC}(q,t)= \begin{cases} t \leq AT(i,1)+ \\ 1 \quad \dfrac{\left[(SOC_r^{\max}-SOC_{initial})\times BC_r+ \left[\left[\dfrac{(DD^{\max}-DD^{\min})}{m_{DD}}\times\dfrac{[(j-1)+j]}{2}+DD^{\min}\right]\times ECPK_r\right]\right]}{R_{Chg}} \\ 0 \quad Otherwise. \end{cases}$$
$$\forall\, t \in \{1,2,...,24\}$$
$$\forall\, q \in \{1,2,...,N_{PS}\}$$
$$j=1:m_{DD} \tag{26}$$

$$PSM_q=\begin{bmatrix}PSM_q(1,:)\\ PSM_q(2,:)\\ PSM_q(3,:)\\ PSM_q(4,:)\end{bmatrix}=\begin{bmatrix}AT(i,1) & AT(i,2)\\ DT(j,1) & DT(j,2)\\ DD(k,1) & DD(k,2)\\ r & \Pr_{type}^{r}\end{bmatrix}_{4\times 2}\begin{matrix}\forall\, q \in \{1,2,...,N_{PS}\}\\ \forall\, i \in \{1,2,...,\tau_{AT}\}\\ \forall\, j \in \{1,2,...,\tau_{DT}\}\\ \forall\, k \in \{1,2,...,m_{DD}\}\\ \forall\, r \in \{1,2,...,N_{PHEV-types}\}\end{matrix} \tag{27}$$

By determining the discussed constraints, the PHEV charging load matrix (PCLM) similar to conventional loads can be calculated by using (28) and (29). In fact, the values of any time corresponding to any state, which can be zero or equal to charging level are added together according to their probability values. Finally, at any time interval, an aggregated PHEV charging load is determined.

$$PCLM(t,1)=\sum_{q=1}^{N_{PS}} R_{Chg}\times\prod_{w=1}^{4} PSM_q(w,2)\times BV_{AT}BV_{DT}BV_{SOC}$$
$$\forall\, t \in \{1,2,...,24\} \tag{28}$$

$$PCLM(t,2)=\frac{1}{24} \quad \forall\, t \in \{1,2,...,24\} \tag{29}$$

2.7. Methodology for Evaluating the Reliability Indices Based on Power Flow Analyses

In order to investigate the reliability indices of the smart grids, it is necessary to evaluate the satisfaction of the power balance condition. In any state of the system, the output power of the renewable DG units e.g. PV-based or WT-based DG units and other non-renewable DG units have been specified. On the other hand, the demand side data is determined by specifying the charging load demand of PHEVs as explained in the previous section and the state of the conventional loads. To take into account the reliability, adequacy, or well-being indices, it is essential to examine the power balance condition under any system state concerning all power flow constraints such as (30)–(32) [45–48].

$$P_{MS}+\sum P_{DGs}-\sum P_{Load}-\sum P_{PHEVs} = \sum_{i=1}^{nbus} V_{q,i}\times V_{q,j}\times Y_{ij}\times\cos(\theta_{ij}+\delta_{q,j}-\delta_{q,i}) \quad \forall\, i,j,\ and\ q \tag{30}$$

$$V_{\min} \leq V_i \leq V_{\max} \quad \forall\, i. \tag{31}$$

$$P_l \leq P_{\max,l} \quad \forall\, l. \tag{32}$$

By performing a simplified power flow under any system state and consideration of the corresponding probability, it is possible to determine the reliability indices. In the proposed model of integration of subsystems and evaluating the reliability indices, a Boolean variable is

Table 3
The main substation states based on its transformer availability

State No.	Number of Out-of-Service Transformers	Available Output Power (p.u)	Probability (%)
1	1	50	3.94
2	2	0	0.02
3	0	100	96.04

Table 2
The data of IEEE 33-bus test system

Line No.	Send Bus	Receive Bus	R (Ω)	X (Ω)	Length (m)	Receive bus peak load demand		Line No.	Send Bus	Receive Bus	R (Ω)	X (Ω)	Length (m)	Receive Bus Peak Load Demand	
						P (kW)	Q (kVAr)							P (kW)	Q (kVAr)
1	1	2	0.0922	0.0470	100	100	60	17	17	18	0.7320	0.5739	700	90	40
2	2	3	0.493	0.2512	500	90	40	18	2	19	0.1640	0.1565	150	90	40
3	3	4	0.3661	0.1864	350	120	80	19	19	20	1.5042	1.3555	1500	90	40
4	4	5	0.3811	0.1941	350	60	30	20	20	21	0.4095	0.4784	400	90	40
5	5	6	0.8190	0.7070	800	60	20	21	21	22	0.7089	0.9373	700	90	40
6	6	7	0.1872	0.6188	200	200	100	22	3	23	0.4512	0.3084	450	90	50
7	7	8	0.7115	0.2351	700	200	100	23	23	24	0.8980	0.7091	900	420	200
8	8	9	1.0299	0.7400	1000	60	20	24	24	25	0.8980	0.7071	900	420	200
9	9	10	1.044	0.7400	1000	60	20	25	6	26	0.2031	0.1034	200	60	25
10	10	11	0.1967	0.0651	200	45	30	26	26	27	0.2842	0.1474	300	60	25
11	11	12	0.3744	0.1298	350	60	35	27	27	28	1.0589	0.9338	1000	60	20
12	12	13	1.4680	1.1549	1500	60	35	28	28	29	0.8043	0.7006	800	120	70
13	13	14	0.5416	0.7129	550	120	80	29	29	30	0.5074	0.2585	500	200	100
14	14	15	0.5909	0.5260	600	60	10	30	30	31	0.9745	0.9629	950	150	70
15	15	16	0.7462	0.5449	750	60	20	31	31	32	0.3105	0.3619	300	210	100
16	16	17	1.2889	1.7210	1300	60	20	32	32	33	0.3411	0.5302	350	60	40

Table 4
DG units Information

DG No.	DG Type	Placement	Rated Capacity capacity (kW)
1	WT	14	400
2	PV	16	500
3	Diesel	17	400
4	WT	20	400
5	PV	21	125
6	Diesel	22	400
7	WT	27	800
8	PV	31	250
9	Diesel	32	800

Table 5
Kyocera–KC200GT Solar Module Data at Standard Test Conditions (STC: $1000W/m^2$Solar Irradiance and$25^{\circ}C$ Module Temperature) [54,55]

Item	Module Characteristics	Value
1	Maximum Power Generation (P_{max}) (W)	200
2	Maximum Power Voltage (V_{mpp}) (V)	35.8
3	Maximum Power Current (I_{mpp}) (A)	7.61
4	Open Circuit Voltage (V_{OC}) (V)	32.9
5	Short Circuit Current (I_{SC}) (A)	8.21
6	Maximum System Voltage (V)	600
7	Power Temperature Coefficient (%/°C)	-0.5
8	Temperature Coefficient of Open Circuit Voltage (mV/°C)	-123
9	Temperature Coefficient of Short Circuit Current (mA/°C)	3.18
10	Nominal Cell Operating Temperature (°C)	47
11	Efficiency (%)	13.9

Table 6
Kyocera–KC200GT Solar Module Data at $47^{\circ}C$Nominal Operating Cell Temperature (NOCT) And $800W/m^2$Solar Irradiance [54, 55]

Item	Module Characteristics	Value
1	Maximum Power Generation (P_{max}) (W)	142
2	Maximum Power Voltage (V_{mpp}) (V)	23.2
3	Maximum Power Current (I_{mpp}) (A)	6.13
4	Open Circuit Voltage (V_{OC}) (V)	29.9
5	Short Circuit Current (I_{SC}) (A)	6.62

Table 7
States of The PV-based DG Units

State No.	Time (hr)	Output Power (p.u)	Probability (%)
1	18 to –6	0	100
2	6 to –9 and 15 to –18	0.1	2.81
3		0.3	38.21
4		0.5	48.33
5		0.7	10.50
6		0.9	0.15
7	9 to –15	0.1	0.25
8		0.3	76.21
9		0.5	23.53
10		0.7	0.01
11		0.9	0.00

defined to investigate the satisfactory of all constraints as (33)–(38). When all power constraints have been met, the discussed Boolean variable is set to 1. Otherwise, the zero value would be assigned. By using the Boolean variable corresponding to the power flow constraints, it is possible to determine the violations of constraints and limits.

$$BV^{q}_{voltage-profile} = \begin{cases} 1 & if\ V_{\min} \le V_i \le V_{\max} \\ 0 & Otherwise. \end{cases} \quad \forall\, i \in \{Buses\} \tag{33}$$

$$BV^{q}_{P-lines} = \begin{cases} 1 & if\ P_{line-i} \le P^{\max}_{line-i} \\ 0 & Otherwise. \end{cases} \quad \forall\, i \in \{Lines\} \tag{34}$$

Table 8
States of The WT-based DG Units

State No.	Wind Speed (m/s)	Output Power (p.u)	Probability (%)
1	<4 or > 25	0	33.53
2	5	0.10	10.69
3	6	0.20	10.01
4	7	0.30	8.99
5	8	0.40	7.80
6	9	0.50	6.57
7	10	0.60	5.38
8	11	0.70	4.31
9	12	0.80	3.37
10	13	0.90	2.59
11	14	1.00	6.77

$$BV^{q}_{P-DGs} = \begin{cases} 1 & if\ P^{\min}_{G,g} \le P_{G,g} \le P^{\max}_{G,g} \\ 0 & Otherwise. \end{cases} \quad \forall\, g \in \{DGs\} \tag{35}$$

$$BV^{q}_{P-D2R} = \begin{cases} 1 & if\ P^{Area}_{DDG} \ge k^{\min}_{D2R} P^{Area}_{DG} \\ 0 & Otherwise. \end{cases} \quad \forall\, g \in \{DGs\} \tag{36}$$

$$BV^{q}_{Constraints} = BV^{q}_{voltage-profile} \times BV^{q}_{P-lines} \times BV^{q}_{P-DGs} \times BV^{q}_{P-D2R} \tag{37}$$

$$BV^{q}_{Constraints} = \begin{cases} 1 & If\ all\ power\ flowconstraints\ have\ been\ satisfied. \\ 0 & Otherwise. \end{cases} \tag{38}$$

The demand side data of conventional loads and PHEVs charging load demand are time-dependent. It means that it is not possible to be available the *t*th state of PHEVs charging load and the *t'*th one of the conventional loads. Furthermore, occurrences of any state of PV-based DG unit is time-dependent. Accordingly, to avoid the producing any unrealistic state in reliability evaluation, the state matrix of time-dependent elements' state (*TDES*) including the data of PV-based DG unit's state (*PVS*), the load state(*LS*), and the PHEV load state (*PLS*)is used as (39) and (40).

$$TDES(j, 1) = PVS(j, 1) - LS\left(floor\left(\frac{j}{\tau_{PV}}\right)\right) - PLS\left(floor\left(\frac{j}{\tau_{PV}}\right)\right) \tag{39}$$

$$TDES(j, 2) = PVS(j, 2) \tag{40}$$

In this paper, the expected energy not-supplied (EENS) is selected as the desired reliability index. The EENS can be calculated by using (41). As shown in (30), the power balance condition and other power flow constraints are considered in order to evaluate the reliability indices.

Moreover, it is possible to evaluate the well-being criteria by using the proposed method and considering the additional constraints that can be found in [12–14,16,49].

$$EENS^{q} = -Min\left\{0, \sum\left[BV^{q}_{Constraints} \times \begin{bmatrix} \sum_{\forall i \in \{1,2,\ldots,N_{WT}\}} WTS(i, 1) + \sum_{\forall j \in \{1,2,\ldots,N_{TR}\}} TRS(j, 1) + \\ \sum_{\forall k \in \{1,2,\ldots,N_{NRES}\}} NRES(k, 1) + \sum_{\forall l \in \{1,2,\ldots,N_{TDE}\}} TDES(l, 1) \end{bmatrix}\right]\right\} \tag{41}$$

After the power flow analyses, the reliability, adequacy, or well-being indices should be calculated for any system state. By aggregating the reliability indices of the system states, the whole system reliability indices can be determined. The weighting coefficients are considered according to the probability of each system state. As can be seen in (42), the whole system EENS as the desired reliability index can be calculated.

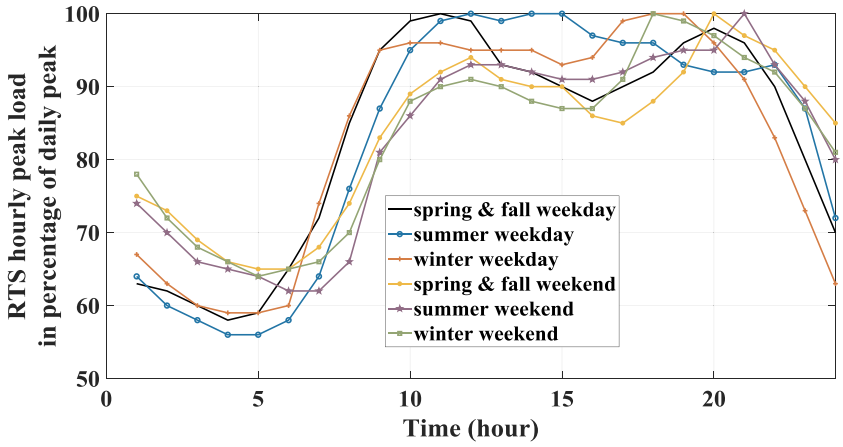

Fig. 6. IEEE-RTS Daily load profiles for working days and weekend days.

Table 9
PHEVs characteristics [16,61]

No.	PHEV Type	ECPK (kWh/km)	Percentage (%)	Battery Capacity (kWh)
1	Compact Sedansedan	0.1625	60.19	10–20
2	Mid-Size Sedan	0.1875	12.04	20–30
3	Mid-Size SUV	0.2375	13.02	30–40
11	Full-Size SUV	0.2875	14.75	40–50

$$EENS = \sum_{q=1}^{N_{SS}} EENS^{q} \times \Pr^{q} \tag{42}$$

3. Test Resultsresults

3.1. Case Study

To illustrate the advantages of the proposed method, it is applied to the IEEE 33-bus test system as can be seen in Fig. 5. The test system data is driven from [35,50] as presented in Table 2.

In the test system, there are 5 protective devices. The protective devices are located upstream of buses 2, 13, 19, 23, and 26. According to the proposed method of modeling the system topology based on the segmentation concept and graph theory, the test system is divided into 5 separate segments as can be seen in Fig. 5.

The failure rate of any segment is calculated based on the summation of the failures of any elements in the segments based on the data reported in [51,52]. It is assumed that the main substation is equipped with two transformers. The various states of the main substation and their probabilities are taken into account by using the failure rate and other data reported in [53] as Table 3.

It is assumed that 9 DG units with 3 types (PV/WT/Diesel-based DG units) are connected to the test system. The placements of these DG units have been shown in Fig. 5. In addition, the other information about the DG units is demonstrated in Table 4.

In this paper, the multi-crystalline modules (Kyocera–KC200GT [54,55]) have been considered for PV-based DG units. The manufacturer data of solar cells are shown in Tables 5 and 6.

Based on the historical data of solar irradiation and clearness index of [56], the aggregated states of the PV-based DG units have been created as Table 7.

Furthermore, the characteristics of WT-based DG units are taken from [8,53]. The wind turbine cut-in, rated, and cut-off speeds are 4, 14, and 25 [57]. The historical and probabilistic data of wind speed in [8] has been used. In Table 8, the states of WT-based DG units are described based on the wind turbine manufacturer characteristics and the historical wind speed data.

Because of the similar behavior of the conventional load under any season [58–60], 8 daily load curves have been considered for working days and weekend days of each season which follow the IEEE-RTS [58]. The different load profiles which follow the IEEE-RTS [58] can be seen in Fig. 6.

The PHEVs types and characteristics are given in Table 9 [16,61]. In this table, the percentage of any PHEV type is noted. In addition, the

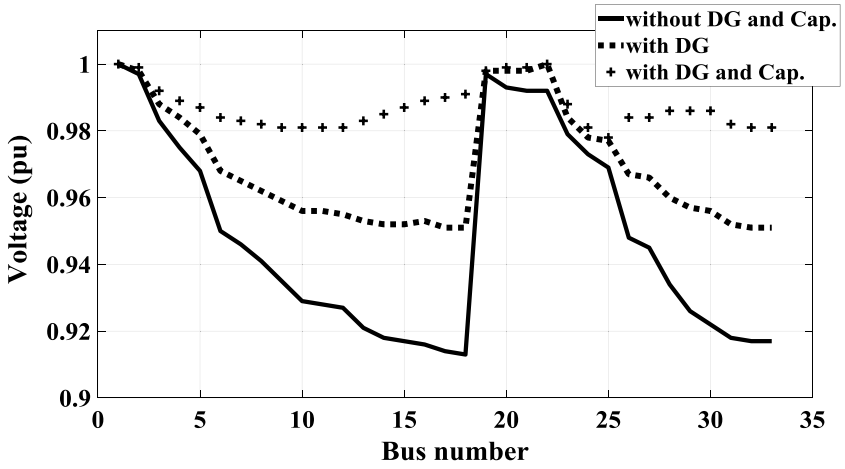

Fig. 7. Voltage profile of buses in different conditions.

Table 10
test results

Reliability/Well-being Indexindex	Proposed Method	MCS like [16]	Method of [9]
EENS (kWh/year)	43234	43373	42793
Healthy State Probability (%)	93.34	95.45	93.41
Duration of Healthy State (hr/year)	8176.65	8361.43	8182.72
Marginal State Probability (%)	5.88	3.77	5.82
Duration of Marginal State (hr/year)	515.07	330.21	509.29
At-Risk State Probability (%)	0.78	0.78	0.77
Duration of At-Risk State (hr/year)	68.28	68.36	67.99

ECPK and the battery size of any PHEV type can be found.

The peak of the PHEVs charging load (maximum demand) was assumed to be 1.6 kW due to simultaneously charging of about 450 PHEVs. Since different charging levels are probable for PHEVs [62–64], in the base condition, it is assumed that 60% of PHEVs are regularly charged, while 30% and 10% of PHEVs are slowly and fast charging.

The voltage profile of any bus of the test system has been shown in Fig. 7. Moreover, in reliability evaluation of any system state, it has been checked that the system meets the power flow constraints e.g. voltage profile.

As described in the previous section, a Boolean variable is defined to investigate the satisfactory of voltage profile constraints as (33). When the voltage profile constraints have been met, the discussed Boolean variable is set to 1. Otherwise, the zero value would be assigned. In this paper, the upper bound and lower bound of the voltage profile of the system buses are assumed to be 1.05 and 0.95 p.u., respectively [65]. It should be noted that in some countries, the different lower and upper bounds of the permitted voltage would be selected. By determining the different upper and lower bounds for voltage limits and other constraints, the power flow constraints satisfactory and reliability calculations would be affected.

The system voltage profile has been analyzed under different conditions such as without any DG and with shunt compensator capacitors, without DG units and without any shunt compensator capacitor, and with DGs and shunt capacitors.

In this paper, it has been assumed that all power flow constraints have been satisfied under the base case. According to the data-driven from [50], some shunt capacitors have been allocated in the test system. As described in [50], the 0.3 MVAr compensating capacitors have been installed in buses 15, 18, 29, and 31. In addition, the 0.6 MVAr capacitors have been installed in bus 30. In this paper, a similar operation condition with small differences has been considered. It has been assumed that the 0.3 MVAr compensating capacitors have been installed in the buses 15, 18, 24, and 30. In addition, the 0.6 MVAr compensating capacitors have been assumed to be installed in buses 6, 10, and 20. The required capacity of the shunt capacitors is a function of the minimum permitted voltage of the buses. The discussed values for capacitors have been determined whereas the minimum magnitude of the buses voltage is considered to be 0.95 p.u. The decrease/increase in the lower bound of the system voltage changes the required capacity of the shunt capacitors.

The voltage profiles of any bus of the system with DG units and with DG units and compensating capacitors are greater than 0.95 p.u. and 0.98 p.u., respectively. According to the consideration of 0.95 p.u. for the minimum permitted voltage, although the compensating capacitors improved the system voltage, the system voltage experiences a normal condition under just installation of DG units. Under conditions that there is no DG unit, the voltage of some buses without reactive power compensation is less than 0.92 p.u. Hence, the use of the compensating capacitors is necessary.

The test results in Fig. 7 have been shown that with compensating capacitors, it is easier to meet the power flow constraint, particularly the voltage limits. In fact, without compensating capacitors, in some conditions, particularly in islanded modes, the system experiences an inadequacy because of the voltage constraint violations. Moreover, when the range of the permitted voltage is extended, the system inadequacy due to the voltage constraints would be decreased.

The satisfactory of both lower and upper bounds are essential. During an operation mode that the maximum permitted voltage condition has not been met, the system experiences a power flow constraint violation. Hence, the system cannot supply the demand loads. The constraint violations due to the under-voltage or over-voltage have similar impacts on the system reliability evaluation.

Usually, the required capacity of shunt capacitors is calculated while the system operates under the inductive condition. As revealed by Fig. 7, the maximum voltage has occurred at bus 1, and the voltage of other buses is less than 1. However, if an over-voltage that exceeds the maximum permitted voltage occurs under eventual special operation

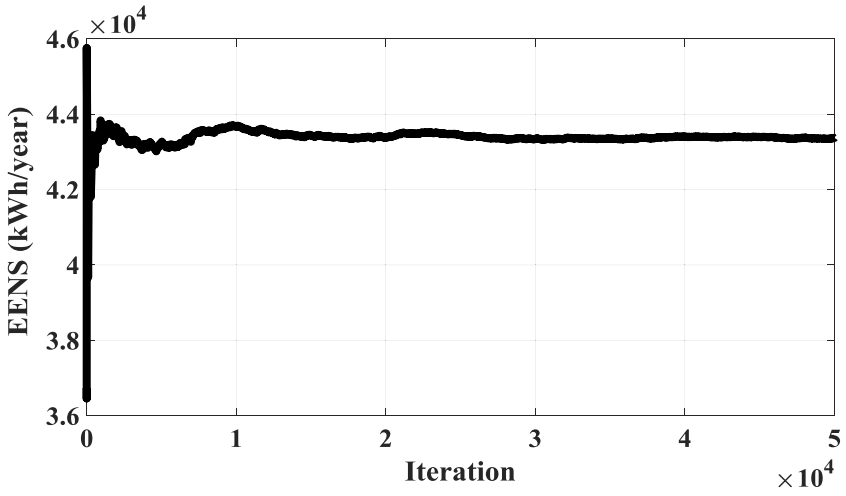

Fig. 8. Convergence diagram of EENS MCS iteration.

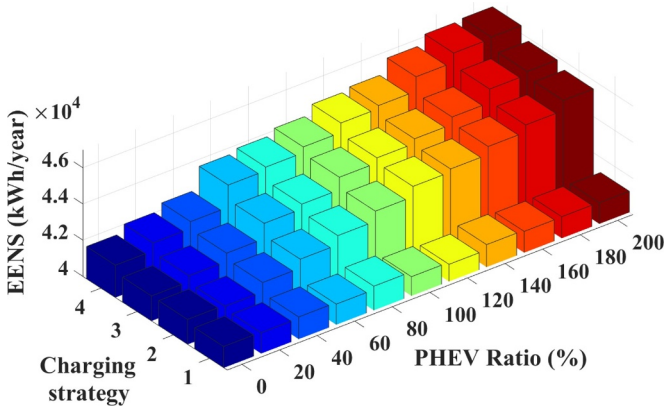

Fig. 9. Sensitivity analysis of EENS due to changes in the PHEVs ratio under different charging level strategies by using the MCS based method of [16].

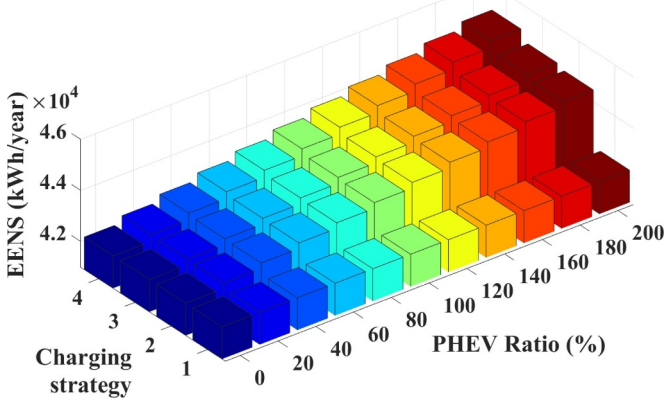

Fig. 10. Sensitivity analysis of EENS due to changes in the PHEVs ratio under different charging level strategies by using the proposed method.

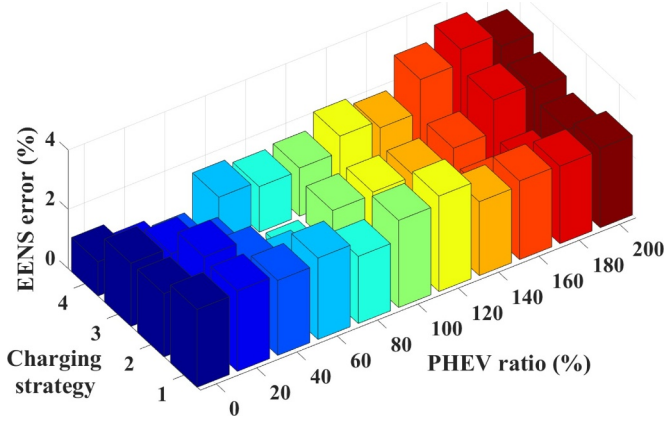

Fig. 11. Sensitivity analysis of EENS inaccuracy by using the proposed method versus the various PHEVs ratio under different charging level strategies.

conditions, a power flow constraint violation has occurred.

In this paper, the grid-connected and islanded modes are considered. In addition, all N-1 contingencies and the corresponding topologies are concerned. When the main substation and segment 1 are available and properly work, the system is operating under the grid-connected mode. Otherwise, the system operates under the islanded mode. Islanded operation modes improve system reliability and decrease EENS.

3.2. Discussion of obtained results and main achievements

In Table 10, the test results obtained based on the proposed generalized reliability evaluation method have been demonstrated. In addition to the EENS, the well-being indices (healthy, marginal, and at-risk probability and duration) have been calculated by using the proposed method.

To validate the test results, the reliability of the test system has been evaluated by using the MCS like [16]. The comparison of the test results based on the proposed method and those of [16] illustrates the accuracy of the proposed method. As revealed by Table 10, the inaccuracy of the reliability index (EENS) due to the discretization of the stochastic states in comparison to MCS-based test results is less than 0.32%. It means that the precise reliability evaluation is achievable by applying the proposed method on the smart grids.

In this paper, the MATLAB has been deployed to implement the proposed reliability evaluation method. In addition, to perform the power flow analysis, the test system has been simulated in DIgSILENT. Moreover, it is possible to develop simplified power flow analysis techniques in MATLAB.

The needed computing time for the proposed method (for MATLAB computations) is about 45 seconds, but the computing time for MCS is about 32,102 seconds while the computer specifications were Intel (R) Core (TM) i7-6700 CPU @ 3.40 GHz 3.40 GHz, RAM 16/0 GB. As shown in Fig. 8, the convergence of the MCS-based method like [16] has appeared in more than 10,000 iterations. Fig. 8 illustrates this fact that the reliability evaluation by MCS in the widespread presence of

Table 11
Test results under different various DG technology scenarios and PHEVs charging strategies

Charging Strategy No.	DG technology Scenario	LOLE (h/year)	EENS (kWh/year)	Period of HealthyState (h/year)	Period of Marginal State (h/year)
1	NRES100	62.69	38534	8371.74	325.57
	WT100	166.15	93742	6038.29	2555.56
	PV100	210.55	134895	4985.70	3563.75
	PV50-WT50	186.78	120307	5519.52	3053.70
	PV20-WT20-NRES60	64.43	39944	8275.21	420.36
	Reference	67.80	42046	8188.14	504.06
	without DG	323.04	240495	2319.44	6117.52
2	NRES100	63.19	39468	8354.98	341.83
	WT100	173.91	98280	5864.89	2721.20
	PV100	210.56	140185	4985.45	3563.99
	PV50-WT50	189.60	125530	5452.74	3117.65
	PV20-WT20-NRES60	64.91	40794	8260.83	434.26
	Reference	68.11	42788	8182.53	509.37
	without DG	323.07	250584	2318.83	6118.11
3	NRES100	63.37	39842	8348.77	347.85
	WT100	173.78	100108	5856.61	2729.61
	PV100	210.58	143248	4984.95	3564.47
	PV50-WT50	189.96	127780	5444.41	3125.63
	PV20-WT20-NRES60	65.04	41139	8256.74	438.22
	Reference	68.27	43093	8179.42	512.31
	without DG	323.10	254890	2318.11	6118.79
4	NRES100	63.66	40115	8341.09	355.26
	WT100	176.09	100902	5813.81	2770.10
	PV100	215.63	144708	4861.24	3683.14
	PV50-WT50	193.16	129620	5366.88	3199.96
	PV20-WT20-NRES60	65.24	41402	8250.75	444.01
	Reference	68.51	43326	8173.97	517.52
	without DG	328.16	258451	2194.11	6237.74

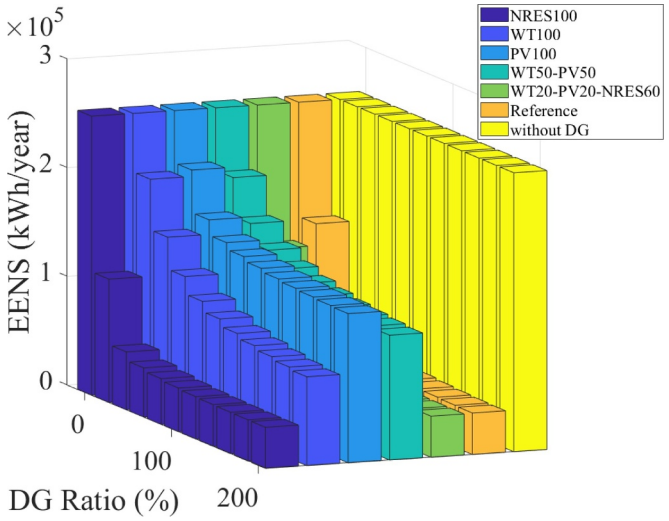

Fig. 12. Sensitivity analysis of EENS due to changes in the DG ratio under different various DG technology scenarios.

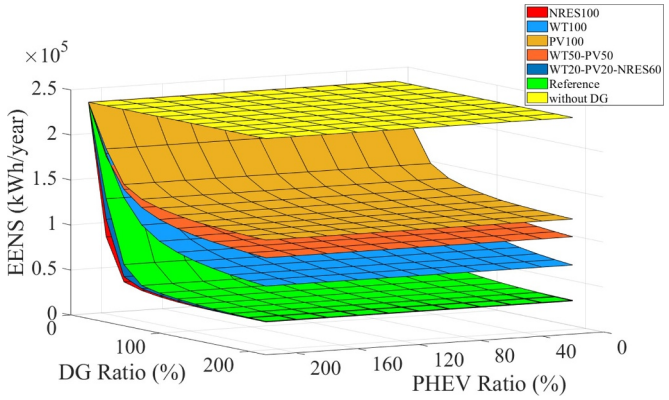

Fig. 13. Sensitivity analysis of EENS due to changes in the PHEVs ratio and DG ratio under the PEHVs charging strategy 1 and various DG technology scenarios.

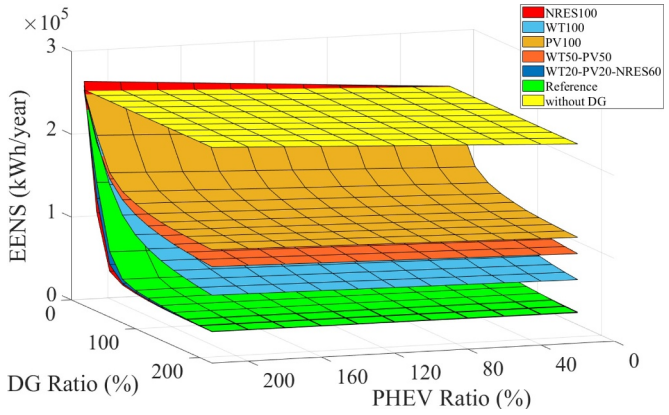

Fig. 14. Sensitivity analysis of EENS due to changes in the PHEVs ratio and DG ratio under the PEHVs charging strategy 2 and various DG technology scenarios.

uncertain parameters in smart grids is time-consuming, and it is very interesting to develop the new precise analytical techniques and methods. The decreasing in computing time of the calculations through the using of the proposed method is significant. Accordingly, applying the presented method is useful and effective when the optimization problems related to improve the reliability of the smart grids is concerned.

Although the compared test results infer that the inaccuracy in the healthy and at-risk state probability is reasonable, the error in marginal state probability due to use of the proposed method in comparison to MCS method [16] is non-negligible. Hence, if it is desired to make a decision about the required reserve and related subjects to the marginal state, it is essential to increase the states and improve the accuracy of the test results.

Because of the advantages of the proposed method in decreasing the computing time, it is possible to perform different sensitivity analyses to get insight into how any parameter affects the system reliability. The sensitivity analysis of EENS due to variation of PHEVs number under different charging level scenarios has been performed to get insight into how the system reliability is affected by PHEVs charging loads. Moreover, the sensitivity analyses are performed in four strategies based on different charging levels [62–64] and seven scenarios based on DG technologies.

The list of PHEVs charging strategies are as follows:

Strategy 1: No charging
Strategy 2: Slow charging
Strategy 3: Regular charging
Strategy 4: Fast charging

In addition, the list of the proposed DG scenarios are as follows:

Scenario 1: reference scenario, the percentage of any DG technology under each segment is considered based on the data of Table 4.
Scenario 2: without DG scenario, there is no DG unit in the system.
Scenario 3: NRES100 scenario, the NRES (non-renewable energy source) type is considered for all DG units.
Scenario 4: WT100 scenario, the WT type is considered for all DG units.
Scenario 5: PV100 scenario, the PV type is considered for all DG units.
Scenario 6: WT50-PV50 scenario, the type of 50% of the DG units is PV and the type of rest ones is WT.
Scenario 7: PV20-WT20-NRES60 scenario, the type of 20%, 20%, and 60% of the DG units is PV, WT, and NRES, respectively.

In Figs. 9 and 10, the PHEVs ratio means a coefficient of any studied case regret to the base case. Furthermore, to strongly validate the proposed method, the discussed sensitivity analysis results were compared by those of the MCS-based method like [16] as shown in Figs. 9 and 10.

As revealed by Fig. 11, the inaccuracies in calculated EENS under different cases and different charging level strategies are less than 3.47%. This comparison results highlight that the proposed method is adequately precise under different conditions.

In addition to the comparison of the obtained results with [9], the test results were compared with those of [9]. The results imply that the error in the reliability index (EENS) due to the assumption of [9] is more than the proposed method. As can be seen, the inaccuracy of the test results (the difference between analytical test results and MCS-based results as reference values) has been improved by applying the proposed method. It seems the methodology of [9] regarding the modeling of the conventional loads leads to increase the inaccuracy. These comparison results emphasized the advantages of the introduced method of this paper. Furthermore, the proposed method is more flexible than [9] to increase the accuracy of the results by increasing the number of states of any system element.

In Table 11, the test results under various DG technology and charging strategies have been presented. The first result of this table that claims the attention is the reliability improvement due to the

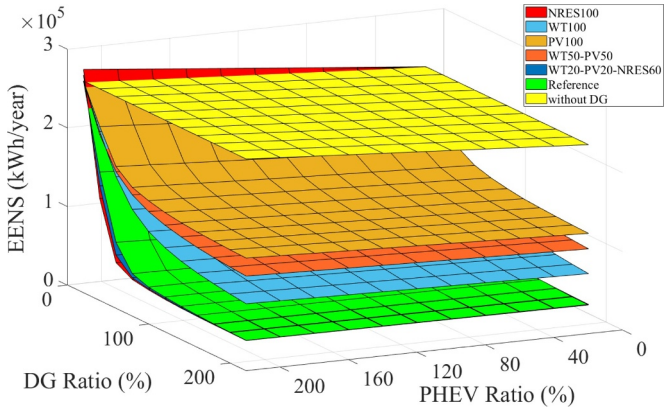

Fig. 15. Sensitivity analysis of EENS due to changes in the PHEVs ratio and DG ratio under the PEHVs charging strategy 3 and various DG technology scenarios.

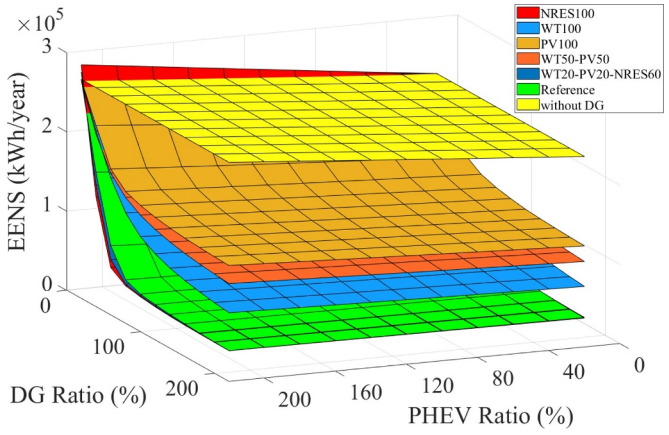

Fig. 16. Sensitivity analysis of EENS due to changes in the PHEVs ratio and DG ratio under the PEHVs charging strategy 4 and various DG technology scenarios.

installation of DG units. The at least 43% improvement in EENS has been achieved by the installation of DG units in comparison with the without DG scenario when there is no PHEV in the system under charging strategy 1. The least effectiveness in reliability improvement under charging strategy 1 belongs to the PV100 scenario. In contrast, the most effective of the discussed charging strategy belongs to the NRES 100 scenario. It means the rated output power of the non-renewable DG units are almost available while the output power of renewable DG units is dependent on uncertain whether parameters.

To illustrate the changes in the system reliability indices such as the EENS, the sensitivity analyses have been performed under various DG technology scenarios via the different penetration levels of DGs. The discussed sensitivity analyses are shown in Fig. 12.

The comparison of the test results under the certain DG technology scenario and different PHEVs charging strategies show that the EENS would be more affected due to the fast charging. The fast charging in comparison to the regular or slow charging strategy leads to an increase in the peak load demand of the PHEVs charging. Therefore, the more inaccuracy due to the increase in the demand side occurs.

In Figs. 13–16, the sensitivity analyses of the EENS due to the changes in the DG and PHEVs ratios under various DG technology scenarios and PHEVs charging strategies have been presented. The obtained results infer that the decrease in the penetration level of DG units leads to an increase in the system EENS. Regardless of the PHEVs charging strategies, the effectiveness of the NRES100 scenario is more than other DG technology scenarios.

As expected, the decrease in the DGs penetration level and the increase in the PHEVs penetration level leads to an increase in the EENS. The comparison of the impacts of the DG and PHEVs penetration levels implies that the system reliability can be more adversely affected due to decrease in the penetration level of DG units in comparison with the increase in the PHEVs penetration level.

4. Conclusion

In this paper, a new generalized analytical reliability assessment method of smart grid was proposed. Proposing a novel methodology based on the segmentation concepts and graph theory for creating the different states of the smart grid is one of the most important contributions. The various operation modes such as the grid-connected and islanding modes are concerned in the introduced topology-based State matrix. Afterward, the State matrix is created for any segment. The state matrix of any segment involving the state of the WT-based DG units, main substation, diesel generators, and time-dependent elements e.g. PV-based DG units, load profile of conventional loads, and the PHEVs charging load demand. One of the most advantages of this paper is developing a new generalized mathematical model for creating the State matrix based on the discretization of the uncertain elements' states. By developing the mathematical model of State matrix of any smart grid element, it is easy to implement any change in the assumptions. Developing a novel mathematical model for PHEVs charging load demand, which considers the manufacturing PHEV data and uncertain parameters of PHEVs' owner behaviors, is another contribution of this article. To evaluate the reliability of the smart grid, the topology State matrix and segments' State matrix are integrated. Accordingly, the reliability indices or well-being criteria can be calculated.

The presented method was applied to the IEEE 33-bus test system. In order to validate the proposed method, the test results have been compared to those of MCS-based methods like [16]. The comparison results illustrated that the introduced method is adequately precise, and it was highlighted that the method of this paper is adequately accurate under different operation scenarios. The test results implied that the speed of the proposed method is about 700 times the MCS-based method of [16]. The significant calculation speed improvement is achievable by applying the proposed method.

In addition, the test results were compared to those of method which reported in [9] as an available analytical model for evaluating the reliability of smart grids. The comparison results emphasized that the proposed method is more accurate.

Decreasing the computing time is another advantage of the proposed method. The introduced method is interesting for using in the sensitivity analyses, optimization problems, etc. because the use of MCS-based approaches under such applications is limited due to their required computing times.

The sensitivity analyses inferred that regardless of the DG technology scenarios, the PHEVs charging strategies affect the system reliability indices such as EENS. Moreover, it can be concluded that it is possible to mitigate the adverse impacts of PHEVs charging on the system reliability by installing the DG units.

References

[1] Acuña LG, Lake M, Padilla RV, Lim YY, Ponzón EG, Soo Too YC. Modelling autonomous hybrid photovoltaic-wind energy systems under a new reliability approach. Energy Convers Manag 2018;172:357–69.
[2] BP.. Bp energy outlook 2018. Tech rep. BP's Energy.
[3] IRENA. Renewable power generation costs in 2017. Abu Dhabi: International Renewable Energy Agency; 2018. 2018.
[4] Conti S, Rizzo SA. Monte Carlo simulation by using a systematic approach to assess distribution system reliability considering intentional islanding. IEEE Trans Power Deliv 2015;30:64–73.
[5] Lei H, Singh C. Non-sequential monte carlo simulation for cyber-induced dependent failures in composite power system reliability evaluation. IEEE Trans Power Syst 2017;32:1064–72.
[6] Urbanucci L, Testi D. Optimal integrated sizing and operation of a CHP system with Monte Carlo risk analysis for long-term uncertainty in energy demands. Energy

Convers Manag 2018;157:307–16.
[7] Atwa YM, El-Saadany EF, Salama MMA, Seethapathy R, Assam M, Conti S. Adequacy evaluation of distribution system including wind/solar DG during different modes of operation. IEEE Trans Power Syst 2011;26:1945–52.
[8] Atwa YM, El-Saadany EF, Guise A. Supply adequacy assessment of distribution system including wind-based DG during different modes of operation. IEEE Trans Power Syst 2010;25:78–86.
[9] Moeini-Aghtaie M, Farzin H, Fotuhi-Firuzabad M, Amrollahi R. Generalized analytical approach to assess reliability of renewable-based energy hubs. IEEE Trans Power Syst 2017;32:368–77.
[10] Falahati B, Fu Y, Wu L. Reliability assessment of smart grid considering direct cyber-power interdependencies. IEEE Trans Smart Grid 2012;3:1515–24.
[11] Falahati B, Fu Y. Reliability assessment of smart grids considering indirect cyber-power interdependencies. IEEE Trans Smart Grid 2014;5:1677–85.
[12] Hashemi-Dezaki H, Askarian-Abyaneh H, Shams-Ansari A, DehghaniSanij M, Hejazi MA. Direct cyber-power interdependencies-based reliability evaluation of smart grids including wind/solar/diesel distributed generations and plug-in hybrid electrical vehicles. Int J Electr Power Energy Syst 2017;93:1–14.
[13] Hashemi-Dezaki H, Askarian-Abyaneh H, Haeri-Khiavi H. Impacts of direct cyber-power interdependencies on smart grid reliability under various penetration levels of microturbine/wind/solar distributed generations. IET Gener Transm Distrib 2016;10:928–37.
[14] Hashemi-Dezaki H, Agah SMM, Askarian-Abyaneh H, Haeri-Khiavi H. Sensitivity analysis of smart grids reliability due to indirect cyber-power interdependencies under various DG technologies, DG penetrations, and operation times. Energy Convers Manag 2016;108:377–91.
[15] Chen C, Wu W, Zhang B, Singh C. An analytical adequacy evaluation method for distribution networks considering protection strategies and distributed generators. IEEE Trans Power Deliv 2015;30:1392–400.
[16] Hashemi-Dezaki H, Hamzeh M, Askarian-Abyaneh H, Haeri-Khiavi H. Risk management of smart grids based on managed charging of PHEVs and vehicle-to-grid strategy using Monte Carlo simulation. Energy Convers Manag 2015;100:262–76.
[17] Billinton B R, Cui Y. Reliability evaluation of small standalone wind energy conversion systems using a time series simulation model. Proc Inst Elect Eng Gen Transm Distrib 2003;150:96–100.
[18] Atashgar K, Abdollahzadeh H. Reliability optimization of wind farms considering redundancy and opportunistic maintenance strategy. Energy Convers Manag 2016;112:445–58.
[19] Volkanovski A. Wind generation impact on electricity generation adequacy and nuclear safety. Reliab Eng Syst Saf 2017;158:85–92.
[20] Eryilmaz S. Reliability analysis of multi-state system with three-state components and its application to wind energy. Reliab Eng Syst Saf 2018;172:58–63.
[21] Eryilmaz S, Devrim Y. Theoretical derivation of wind plant power distribution with the consideration of wind turbine reliability. Reliab Eng Syst Saf 2019;185:192–7.
[22] Li H, Wang X, Gao Y, Liang H. Evaluation research of the energy supply system in multi-energy complementary park based on the improved universal generating function method. Energy Convers Manag 2018;174:955–70.
[23] Nojavan S, Aalami Ha. Stochastic energy procurement of large electricity consumer considering photovoltaic, wind-turbine, micro-turbines, energy storage system in the presence of demand response program. Energy Convers Manag 2015;103:1008–18.
[24] Souloukngа MH, Doka SY, Revanna N, Djongyang N, Kofane TC. Analysis of wind speed data and wind energy potential in Faya-Largeau, Chad, using Weibull distribution. Renew Energy 2018;121:1–8.
[25] Wang L, Yuan J, Cholette ME, Fu Y, Zhou Y, Tan AC. Comparative study of discretization method and Monte Carlo method for wind farm layout optimization under Weibull distribution. J Wind Eng Ind Aerodyn 2018;180:148–55.
[26] Samal RK, Tripathy M. Cost savings and emission reduction capability of wind-integrated power systems. Int J Electr Power Energy Syst 2019;104:549–61.
[27] Ayvazoğluyüksel Ö, Filik ÜB. Estimation methods of global solar radiation, cell temperature and solar power forecasting: a review and case study in Eskişehir. Renew Sustain Energy Rev 2018;91:639–53.
[28] Xiao C, Yu X, Yang D, Que D. Impact of solar irradiance intensity and temperature on the performance of compensated crystalline silicon solar cells. Sol Energy Mater Sol Cells 2014;128:427–34.
[29] Cortés A, Mazón J, Merino J. Strategy of management of storage systems integrated with photovoltaic systems for mitigating the impact on LV distribution network. Int J Electr Power Energy Syst 2018;103:470–82.
[30] Rathore A, Patidar NP. Reliability assessment using probabilistic modelling of pumped storage hydro plant with PV-Wind based standalone microgrid. Int J Electr Power Energy Syst 2019;106:17–32.
[31] Munkhammar J, Widén J. Correlation modeling of instantaneous solar irradiance with applications to solar engineering. Sol Energy 2016;133:14–23.
[32] Linguet L, Pousset Y, Olivier C. Identifying statistical properties of solar radiation models by using information criteria. Sol Energy 2016;132:236–46.
[33] Li Y-F, Zio E. A multi-state model for the reliability assessment of a distributed generation system via universal generating function. Reliab Eng Syst Saf 2012;106:28–36.
[34] Zubo RHA, Mokryani G, Abd-Alhameed R. Optimal operation of distribution networks with high penetration of wind and solar power within a joint active and reactive distribution market environment. Appl Energy 2018;220:713–22.
[35] Ali A, Raisz D, Mahmoud K. Optimal oversizing of utility-owned renewable DG inverter for voltage rise prevention in MV distribution systems. Int J Electr Power Energy Syst 2019;105:500–13.
[36] Rocchetta R, Li YF, Zio E. Risk assessment and risk-cost optimization of distributed power generation systems considering extreme weather conditions. Reliab Eng Syst Saf 2015;136:47–61.
[37] Di Somma M, Graditi G, Heydarian-Forushani E, Shafie-khah M, Siano P. Stochastic optimal scheduling of distributed energy resources with renewables considering economic and environmental aspects. Renew Energy 2018;116:272–87.
[38] Faza A. A probabilistic model for estimating the effects of photovoltaic sources on the power systems reliability. Reliab Eng Syst Saf 2018;171:67–77.
[39] Shafiee S, Fotuhi-Firuzabad M, Rastegar M. Investigating the impacts of plug-in hybrid electric vehicles on power distribution systems. IEEE Trans Smart Grid 2013;4:1351–60.
[40] Wang X, Karki R. Exploiting PHEV to augment power system reliability. IEEE Trans Smart Grid. 2017;8:2100–8.
[41] Li Y, Xie K, Wang L, Xiang Y. The impact of PHEVs charging and network topology optimization on bulk power system reliability. Electr Power Syst Res 2018;163:85–97.
[42] Lee T, Bareket Z, Gordon T, Filipi ZS. Stochastic modeling for studies of real-world PHEV usage: driving schedule and daily temporal distributions. IEEE Trans Veh Technol 2012;61:1493–502.
[43] Maria Luisa Di Silvestre ERS, Zizzo Gaetano, Graditi Giorgio. An optimization approach for efficient management of EV parking lots with batteries recharging facilities. J Ambient Intell Hum Comput 2013;4:641–9.
[44] Kheradmand-Khanekehdani H, Gitizadeh M. Well-being analysis of distribution network in the presence of electric vehicles. Energy 2018;155:610–9.
[45] Wang Q, Liao J, Su Y, Lei C, Wang T, Zhou N. An optimal reactive power control method for distribution network with soft normally-open points and controlled air-conditioning loads. Int J Electr Power Energy Syst 2018;103:421–30.
[46] Esmaeili S, Anvari-Moghaddam A, Jadid S, Guerrero JM. Optimal simultaneous day-ahead scheduling and hourly reconfiguration of distribution systems considering responsive loads. Int J Electr Power Energy Syst 2019;104:537–48.
[47] Sadati SMB, Moshtagh J, Shafie-khah M, Catalão JPS. Smart distribution system operational scheduling considering electric vehicle parking lot and demand response programs. Electr Power Syst Res 2018;160:404–18.
[48] Arefifar SA, Mohamed YAI. DG Mix, reactive sources and energy storage units for optimizing microgrid reliability and supply security. IEEE Trans Smart Grid 2014;5:1835–44.
[49] Billinton R, Karki R. Reliability/cost implications of utilizing photovoltaics in small isolated power systems. Reliab Eng Syst Saf 2003;79:11–6.
[50] Saonerkar AK, Bagde BY.Optimized DG placement in radial distribution system with reconfiguration and capacitor placement using genetic algorithm. 2014IEEE international conference on advanced communications, Control and Computing Technologies 2014. p. 1077-1083.
[51] AlMuhaini M, Heydt G. A novel method for evaluating future power distribution system reliability. IEEE PES general meeting | conference & exposition. 2014. p. 1.
[52] Qi Y, Wang F, Wang D. Reliability analysis of distribution system with DG considering operation homogeneity. China international conference on electricity distribution (CICED). 2016. p. 1–5.
[53] Hamzeh M, Vahidi B, Askarian-Abyaneh H. Reliability evaluation of distribution transformers with high penetration of distributed generation. Int J Electr Power Energy Syst 2015;73:163–9.
[54] Data sheet of KC200GT,https://www.kyocerasolar.com/dealers/product-center/archives/spec-sheets/KC200GT.pdf.
[55] Babu C, Ponnambalam P. The theoretical performance evaluation of hybrid PV-TEG system. Energy Convers Manag 2018;173:450–60.
[56] University of Washington, Seattle, “Power Systems Test Case Archive,” 2016. [Online]. Available:http://www2.ee.washington.edu/research/pstca/.
[57] Aghbalou N, Charki A, Elazzouzi SR, Reklaoui K. A probabilistic assessment approach for wind turbine-site matching. Int J Electr Power Energy Syst 2018;103:497–510.
[58] Subcommittee PM. IEEE reliability test system. IEEE Trans Power Appar Syst 1979;PAS-98:2047–54.
[59] Saeed Hasanvand MN, Fallahzadeh-Abarghouei Hossein. A new distribution power system planning approach for distributed generations with respect to reliability assessment. J Renew Sustain Energy 2016:8.
[60] Oviedo RM, Fan Z, Gormus S, Kulkarni P. A residential PHEV load coordination mechanism with renewable sources in smart grids. Int J Electr Power Energy Syst 2014;55:511–21.
[61] Ma T, Mohammed OA. Economic analysis of real-time large-scale PEVs network power flow control algorithm with the consideration of V2 G services. IEEE Trans Ind Appl 2014;50:4272–80.
[62] Sehar F, Pipattanasomporn M, Rahman S. Demand management to mitigate impacts of plug-in electric vehicle fast charge in buildings with renewables. Energy 2017;120:642–51.
[63] Gnann T, Funke S, Jakobsson N, Plötz P, Sprei F, Bennehag A. Fast charging infrastructure for electric vehicles: today's situation and future needs. Transp Res Part D 2018;62:314–29.
[64] Jalilzadeh Hamidi R, Livani H. Myopic real-time decentralized charging management of plug-in hybrid electric vehicles. Electr Power Syst Res 2017;143:522–32.
[65] Aman MM, Jasmon GB, Bakar AHA, Mokhlis H. A new approach for optimum DG placement and sizing based on voltage stability maximization and minimization of power losses. Energy Convers Manag 2013;70:202–10.